Approximation of excitonic absorption in disordered systems using a compositional-component-weighted coherent-potential approximation

N. F. Schwabe and R. J. Elliott
Department of Physics, University of Oxford, Theoretical Physics, 1 Keble Road, Oxford OX1 3NP, United Kingdom
(Received 17 August 1995; revised manuscript received 10 November 1995)

Employing a recently developed technique of component-weighted two-particle Green's functions in the coherent-potential approximation (CPA) of a binary substitutional alloy A_cB_{1-c} we extend the existing theory of excitons in such media using a contact potential model for the interaction between electrons and holes to an approximation which interpolates correctly between the limits of weak and strong disorder. With our approach we are also able to treat the case where the contact interaction between carriers varies between sites of different types, thus introducing further disorder into the system. Based on this approach we study numerically how the formation of exciton bound states changes as the strengths of the contact potentials associated with either of the two site types are varied through a large range of parameter values.

I. INTRODUCTION

Excitonic optical absorption in strongly disordered semiconductor alloys has been of great interest to both semiconductor physics and technological applications of semiconductors and semiconductor structures in the past. Although the theory of an optically excited electron-hole pair scattered or bound under the influence of the mutual Coulomb interaction into an exciton is quite well understood in weakly disordered systems and even at finite carrier densities in the respective conduction and valence bands, theories for strongly disordered systems such as alloys of insulators and some semiconductors are still very incomplete.

One of the few theories of disorder which interpolates correctly between all regimes of disorder strengths and concentrations is the coherent-potential approximation (CPA) first developed by Soven[1] and Taylor [2] and subsequently extended to a proper two-particle theory by Velicky.[3] The CPA predicts correctly the occurrence of splitoff impurity bound states and whole impurity bands, once the relative disorder strength becomes of the order of the width of the unperturbed single-particle density of states considered. Despite the numerous advantages that the CPA provides, it has proved difficult to incorporate a treatment of a carrier-carrier interaction into its framework and to our knowledge the only attempt to find a joint treatment of both effects has been made by Kanehisa and Elliott[4] who introduced a random-phase-like decoupling of the disorder average in the corresponding perturbation expansion in combination with a contact potential model for the Coulomb interaction. Although this description produces a number of correct features in a limit of low disorder, it could not be extrapolated successfully to the case where the disorder becomes stronger, i.e., when the joint density of states splits into two components and the excitons move to a more localized Frenkel limit, where a separate approach is needed. No theory has been available for the region of intermediate disorder strengths where the bands are about to split.

An improved treatment of this problem has become possible through the development of a properly weighted two-particle CPA in a previous paper[5] which allows one to distinguish between different site types involved in the propagation of two-particles during an absorption process. We will show that differentiating between alloy components in a perturbation expansion with an appropriate decoupling procedure of the disorder average can yield the correct interpolation to all ranges of disorder for a contact potential model. Furthermore, this allows us to distinguish different contact interaction strengths between the carriers if these meet on different types of sites, due to different dielectric constants in the respective materials, whereby these strengths are modeled to represent the electron-hole interaction within an atomic radius.

II. ABSORPTION IN THE NONINTERACTING DISORDERED ALLOY

A. CPA model of the disordered system

We summarize here the results for a component-weighted two-particle CPA. Our model system is a binary substitutional alloy of components A and B with respective concentrations c and $1-c$, on a simple three-dimensional monoatomic lattice. Both components are assumed to exhibit a direct band gap in their pure phase. Our two-band model Hamiltonian without carrier-carrier interactions can thus be written in a site representation as

$$H=\sum_{l,n}\{W_l^c c_{n+l}^{+}c_n+W_l^v d_{n+l}^{+}d_n\}+\sum_n\{U_n^c c_n^{+}c_n+U_n^v d_n^{+}d_n\}, \tag{1}$$

where the c_n and d_n are the annihilation operators for an electron and a hole on the site n, respectively. W^μ is the periodic part of the Hamiltonian transferring particles between different sites in the band μ and U_n^μ is the matrix element in the respective bands which assumes the values $U_n^\mu\in\{\varepsilon_A^\mu,\varepsilon_B^\mu\}$ depending on whether n is an A or a B site. The disorder in the system is generated by the difference of the on-site energies $V^\mu=\varepsilon_A^\mu-\varepsilon_B^\mu$ in the respective bands.

The CPA for a disordered medium is introduced by the usual method[1,2,6] of placing the impurities in a self-consistent medium such that the scattering off a single impurity vanishes on the average. Independent of this approximation, the single-particle propagator of the disordered medium G relates to the one of a pure medium g through the Dyson equation

$$G^{\mu}=g^{\mu}+g^{\mu}U^{\mu}G^{\mu}. \tag{2}$$

The the self-consistent CPA condition requires that the average propagator $\bar{G}^{\mu}$ of the effective medium fulfill the relation

$$\bar{G}^{\mu}=g^{\mu}+g^{\mu}\Sigma^{\mu}\bar{G}^{\mu}, \tag{3}$$

where Σ^{μ} is the CPA single-particle self-energy of the effective medium. Σ^{μ} itself is determined through the single-site condition that the average atomic T matrix of the self-consistent medium T_n^{μ} defined as

$$T_n^{\mu}=(U_n^{\mu}-\Sigma^{\mu})+(U_n^{\mu}-\Sigma^{\mu})F^{\mu}T_n^{\mu}, \tag{4}$$

be zero. Here we have introduced the site diagonal single-particle function $F=\bar{G}(n,n)$. Σ^{μ} and F^{μ} therefore satisfy the self-consistent relation

$$0\equiv\langle T_n^{\mu}\rangle=\frac{c[\varepsilon_A^{\mu}-\Sigma^{\mu}]}{1-[\varepsilon_A^{\mu}-\Sigma^{\mu}]F^{\mu}}+\frac{(1-c)[\varepsilon_B^{\mu}-\Sigma^{\mu}]}{1-[\varepsilon_B^{\mu}-\Sigma^{\mu}]F^{\mu}}. \tag{5}$$

Weights can now be attributed to the single-particle functions before averaging through applying operators $\Xi_{\mu}^{i/h}$ to them which effectively exclude either impurity or host sites from the choices of start or end sites of the propagation of the particles. We make the following definitions:

$$\Xi_{\mu}^{A}=[U_n^{\mu}-\varepsilon_B^{\mu}]/V^{\mu},\quad G^{A}=\Xi_{\mu}^{A}G,\quad G^{AA}=\Xi_{\mu}^{A}\,G_{\mu}\Xi_{\mu}^{A},$$

$$\Xi_{\mu}^{B}=[\varepsilon_A^{\mu}-U_n^{\mu}]/V^{\mu},\quad G^{B}=\Xi_{\mu}^{B}G,\quad G^{BB}=\Xi_{\mu}^{B}G_{\mu}\Xi_{\mu}^{B},$$

$$G^{AB}=\Xi_{\mu}^{A}G_{\mu}\Xi_{\mu}^{B},\quad G^{BA}=\Xi_{\mu}^{B}G_{\mu}\Xi_{\mu}^{A}. \tag{6}$$

Averaged versions of such weighted single-particle functions have been introduced by Aiyer *et al.*[7] It will be shown that they are particularly useful in their unaveraged form when employed in the definitions of two-particle functions in order to calculate weighted components of the polarizability which can thereupon be used in the treatment of the excitonic absorption.

B. The average polarizability in linear response theory

In the following we consider a linear response expression for the polarizability of the Kubo type. The particular kind of two-particle function needed in this case is determined by the form of the dipole operators which account for the interaction of the electronic excitation with the radiation field and which in the case of allowed interband transitions[8] effectively couple the two single-particle resolvents in the respective bands:

$$\hat{\mathbf{p}}^{\dagger}=\sum_n |nc\rangle p\langle nv|. \tag{7}$$

The total optical polarizability in a Matsubara representation which we adopt for convenience can be written as

$$\langle\Pi_0(i\omega)\rangle=-\beta^{-1}\sum_{iz}\langle\mathrm{Tr}_v\{\hat{\mathbf{p}}G_c(iz)\hat{\mathbf{p}}^{\dagger}G_v(i\omega-iz)\}\rangle, \tag{8}$$

where the angular brackets denote the configurational average, β is the usual inverse temperature and Tr_v denotes the trace over the band v as in Ref. 9:

$$\mathrm{Tr}_v(\cdots)=\sum_n\langle nv|\cdots|nv\rangle. \tag{9}$$

Here it is assumed that the dipole matrix elements are taken for the transition from a valence band of p-wave symmetry to a conduction band of s-wave symmetry in which case they can be assumed to be essentially constant and we normalize them to unity. This implies that for the calculation of a properly averaged polarizability which is void of any further interactions we need to consider the following two-particle function:

$$K(z_1,z_2)=\sum_m K(z_1,z_2;n,m)=\sum_m\langle nc|\langle G_c(z_1)|mc\rangle \times\langle mv|G_v(z_2)\rangle|nv\rangle. \tag{10}$$

Apart from the cumulative function K stated above it is now also possible to consider its weighted components by using the appropriately weighted versions of the single-particle functions in their definitions.

K and its weighted versions are obtained by means of the two-particle extension of the CPA by Velický[3] and our method of obtaining the appropriate weights.[5] The concept is to use the T matrix representation of the unaveraged unweighted or weighted single particle functions from (6) to obtain a CPA vertex correction $\Lambda(z_1,z_2)$ and average weights for the correlated motion of two-particles in terms of averages over products of atomic T matrices. With the vertex correction, the equation for the correlated two-particle motion can be decoupled as

$$K(z_1,z_2)=\frac{R(z_1,z_2)}{1-\Lambda(z_1,z_2)R(z_1,z_2)}, \tag{11}$$

where $R(z_1,z_2)$ is the average-decoupled two-particle function

$$R(z_1,z_2)=\sum_m\bar{G}_c(z_1;n,m)\bar{G}_v(z_2;m,n) \tag{12}$$

and the vertex correction is found to be

$$\Lambda(z_1,z_2)=\frac{V_v\Sigma_c(z_1)-V_c\Sigma_v(z_2)}{V_cF_c(z_1)-V_vF_v(z_2)}. \tag{13}$$

If one assumes that the conduction and valence band dispersions are similar in shape

$$\frac{\varepsilon_c(k)}{w_c}=\mp\frac{\varepsilon_v(k)}{w_v}, \tag{14}$$

one finds a more explicit representation for $R(z_1,z_2)$ Ref. 9

$$R(z_1,z_2)=\frac{w_cF_c(z_1)\pm w_vF_v(z_2)}{w_c[z_2-\Sigma_v(z_2)]\pm w_v[z_1-\Sigma_c(z_1)]}. \quad (15)$$

In Ref. 5 we found that for the class of two-particle functions as represented by $K(z_1,z_2)$ two types of single-weighted functions and three different double-weighted ones exist. Similar to the single-particle theory it was found that these weighted two-particle functions can be expressed in terms of the unweighted one if energy dependent weighting factors added to and multiplied onto it.

Introducing

$$\xi(z_1,z_2)=\frac{(1-c)\Lambda(z_1,z_2)}{[V_c-\Sigma_c(z_1)][V_v-\Sigma_v(z_2)]}, \quad (16)$$

$$\eta(z_1,z_2)=\frac{c\Lambda(z_1,z_2)}{\Sigma_c(z_1)\Sigma_v(z_2)}, \quad (17)$$

$$\gamma(z_1,z_2)=\frac{\Lambda(z_1,z_2)F_c(z_1)F_v(z_2)}{V_cV_v}, \quad (18)$$

we find that

$$K^A=\xi K, \quad K^B=\eta K, \quad K^{AA}=\xi^2K+\gamma, \quad K^{BB}=\eta^2K+\gamma,$$

$$K^{AB}=K^{BA}=\xi\eta K-\gamma. \quad (19)$$

These functions can now readily be used to obtain corresponding components of the polarizability which are calculated the same way as in (8)

$$\langle\Pi_0^{XY}(i\omega)\rangle=-\beta^{-1}\sum_{iz}K^{XY}(iz,i\omega-iz), \quad (20)$$

where X and Y denote possible weights ($X,Y\in\{A,B,\varnothing\}$). Functions of this type have been discussed analytically and numerically in Ref. 5 for various regimes of disorder.

III. INTRODUCTION OF ELECTRON-HOLE INTERACTION

A. Difficulties with the treatment of the Coulomb interaction in disordered systems

The inclusion of a carrier-carrier interaction into a model for the optical polarizability is essential for the treatment of exciton effects. However, an analytic treatment of this problem in strongly disordered systems such as alloys of insulators and of semiconductors using the true or screened Coulomb interaction seems to be almost impossible. This is due to the fact that the corresponding Bethe-Salpeter equation,

$$\langle\mathscr{K}(i\omega;i,j;k,l)\rangle=\langle\mathscr{K}_0(i\omega;i,j;k,l)\rangle + \sum_{a,b,c,d}\langle\mathscr{K}_0(i\omega;i,j;a,b)u(a,b;c,d) \times\mathscr{K}(i\omega;c,d;k,l)\rangle, \quad (21)$$

is extremely hard to decouple. Here $u(a,b;c,d)=v(a-b)\delta_{ac}\delta_{bd}-w(a-c)\delta_{ab}\delta_{cd}$ is the Coulomb interaction in the site representation with its direct and exchange part and $\mathscr{K}_0(i\omega;i,j;k,l)$ is the noninteracting configuration dependent two-particle function

$$\mathscr{K}_0(i\omega;i,j;a,b)=-\beta^{-1}\sum_{i\omega}\langle i|G_c(iz)|k\rangle\langle l|G_v(iz-i\omega)|j\rangle. \quad (22)$$

The exactly averaged polarizability including exciton effects is calculated from the interacting version of this function (21) as

$$\langle\Pi(i\omega)\rangle=\sum_{i,k}\langle\mathscr{K}(i\omega;i,i;k,k)\rangle. \quad (23)$$

The main difficulty in solving Eq. (21) arises from the fact that the disorder average over the second term creates higher order correlations in the particle motion than those which are accounted for by the inclusion of the vertex corrections. These additional average induced correlations lead to an effective Coulomb interaction which is renormalized in a very complicated fashion.

For these reasons two drastic simplifications have been made in earlier treatments of the problem. First the Coulomb interaction is replaced by a short range contact potential which binds at most one state in a joint band limit when the disorder is relatively weak. This state is meant to represent the 1-s exciton from the Coulomb series which usually dominates the optical absorption spectrum below the continuum absorption edge. Second the disorder average in (21) is decoupled into a product of averages. The average polarizability including this carrier-carrier interaction is then obtained as

$$\overline{\Pi}(i\omega)=\frac{\overline{\Pi}_0(i\omega)}{1+u\overline{\Pi}_0(i\omega)}, \quad (24)$$

where u is the uniform strength of the contact potential and the average was replaced through a horizontal bar over corresponding quantities. However, this type of decoupling of the average becomes reasonable only in the limit of weak disorder, when the electron-hole pair experiences many impurities before its constituents are Coulomb scattered (Wannier excitons). Effectively, therefore no higher than two-particle correlations can be accounted for within this approximation and it will be shown that for stronger disorder even these correlations are significantly misweighted and overcounted. It hence must clearly fail in a regime of strong disorder where excitons may be primarily associated with two separate impurity bands.

For the strong disorder limit it is shown explicitly in Ref. 4 how the solution for the two-particle function is modified towards a regime of localized excitations (Frenkel excitons), which is equivalent to letting the overlap of the atomic wave functions go to zero, while at the same time the disorder strengths are kept constant. If (21) is considered before averaging in this limit, it goes over to

$$[1+\pi_0(i\omega;i)v(0)]\mathscr{K}(i\omega;ii,kk) =\delta_{ik}\pi_0(i\omega;i)+\pi_0(i\omega;i)\sum_j w(i-j)\mathscr{K}(i\omega;jj,kk), \quad (25)$$

where $\pi_0(i\omega;i)$ is the atomic polarizability on the site i and $w(i-j)$ is the exchange part of the Coulomb interaction

which is now entirely responsible for electron transfer from one atom to another. It is this term which makes an exact solution of Eq. (25) still difficult. If now the exchange w is assumed to go to zero as well we obtain the limit of isolated atoms.

The solution of (25) then becomes

$$\mathscr{K}(i\omega;ii,kk)=\frac{\delta_{ik}\pi_0(i\omega,i)}{1+v(0)\pi_0(i\omega,i)}, \tag{26}$$

which can be averaged exactly and summed to yield

$$\overline{\Pi}(i\omega)=\left[\frac{c\,\pi_0(i\omega,A)}{1+v(0)\pi_0(i\omega,A)}+\frac{(1-c)\pi_0(i\omega,B)}{1+v(0)\pi_0(i\omega,B)}\right], \tag{27}$$

where A and B within π_0 denote here that the atomic polarizabilities are considered on either an A or a B atom. Since the present limit corresponds to letting the bandwidth of the components of the joint density of states go to zero, given some arbitrary strength of disorder, the same limiting behavior of the polarizability can be attained[5] by letting the disorder strengths become much larger than the bandwidth which yields two energetically separated contributions to the joint density of states (DOS) and the formal properties of (27) are recovered.

The appearance of (27) suggests that one should also allow for the possibility of using two different contact interaction strengths on different types of sites thus allowing for different types of atomic screening in different alloy components.

It is clear that Eq. (27) is not obtained by the extrapolation to a strong disorder limit from Eq. (24) and so far there had been no indication as to what type of approximation one should use in the description of an intermediate disorder regime, where the strengths of the disorder V_μ are of the order of the corresponding half-widths of the single particle bands w_μ, which at the same time extrapolates correctly to the asymptotic behavior predicted by Eqs. (24) and (27) for weak and strong disorder, respectively.

B. Component-weighted approximation of the scattering expansion

Based on our results in Ref. 5 we employ in the following a component-weighted scattering expansion to obtain the excitonic polarizability, while at the same time we allow the contact potential strengths to assume different values on different types of sites. We use a similar decoupling of the disorder averages to obtain a new approximation for the scattering in an intermediate disorder regime. Subsequently, we show that this approximation renders exactly the interpolation behavior that we had hoped to achieve.

We introduce the following attractive weighted contact scattering interaction strengths

$$\tilde{u}_A=\frac{u_A}{c},\quad \tilde{u}_B=\frac{u_B}{1-c}, \tag{28}$$

associated with the A and B components of the medium, whereby u_A and u_B represent bare scattering strengths, and the limit of uniform interaction strengths corresponds to $u_A\to u_B\to u$. If one distinguishes now the different types of sites involved in the propagation of the two-particles during a scattering process, the expansion of the scattering series can be represented pictorially as in Fig. 1. Mathematically this corresponds to writing

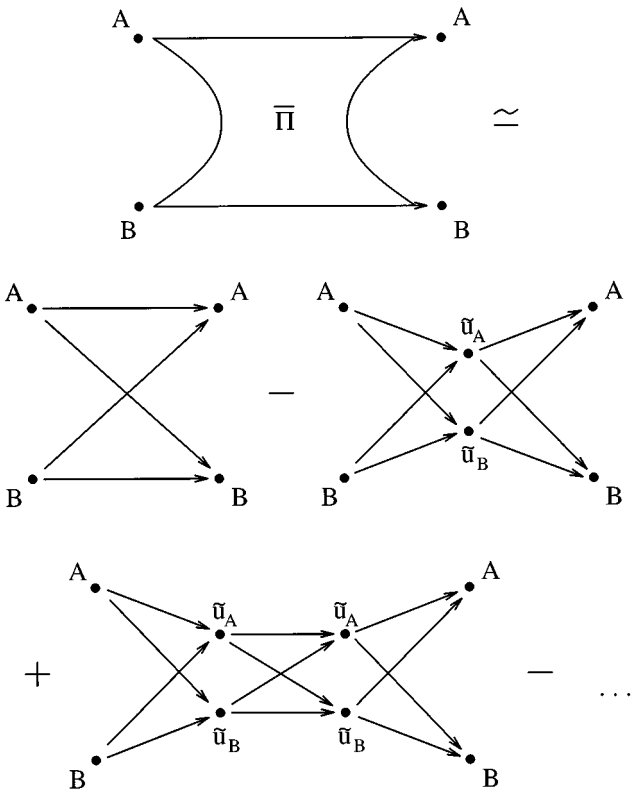

FIG. 1. Diagrammatic representation of processes to second order included in the weighted expansion of the excitonic polarizability. The electron-hole pair can be excited on an A or a B site and subsequently be scattered on either of such sites with the effective contact potential strengths $\tilde{u}_A$ and $\tilde{u}_B$, respectively. Every connecting line between two sites denotes a factor of a noninteracting weighted polarizablity $\overline{\Pi}_0^{XY}$ $(X,Y\in\{A,B\})$, where X and Y are chosen to match the type of the start and the end site of an arrow and all conceivable paths occurring between the excitation and the recombination of the electron-hole pair are being summed over.

$$\begin{aligned}\overline{\Pi}\simeq{}&\overline{\Pi}_0^A+\overline{\Pi}_0^B-[\overline{\Pi}_0^A\tilde{u}_A\overline{\Pi}_0^A+\overline{\Pi}_0^B\tilde{u}_B\overline{\Pi}_0^B]+[\overline{\Pi}_0^A\tilde{u}_A\overline{\Pi}_0^{AA}\tilde{u}_A\overline{\Pi}_0^A\\&+\overline{\Pi}_0^A\tilde{u}_A\overline{\Pi}_0^{AB}\tilde{u}_B\overline{\Pi}_0^B+\overline{\Pi}_0^B\tilde{u}_B\overline{\Pi}_0^{AB}\tilde{u}_A\overline{\Pi}_0^A+\overline{\Pi}_0^B\tilde{u}_B\overline{\Pi}_0^{BB}\tilde{u}_B\overline{\Pi}_0^B]\\&-\cdots,\end{aligned} \tag{29}$$

where both, the diagrams in Fig. 1 and the terms written down in (29) above represent the expansion to second order. These and higher order terms can can be conveniently rewritten in a 2×2 matrix scattering formalism by introducing

$$\vec{\Pi}_0=\begin{pmatrix}\overline{\Pi}_0^A\\ \overline{\Pi}_0^B\end{pmatrix},\quad \hat{\mathbf{U}}=\begin{pmatrix}-\tilde{u}^A & 0\\ 0 & -\tilde{u}^B\end{pmatrix},\quad \hat{\Pi}_0=\begin{pmatrix}\overline{\Pi}_0^{AA} & \overline{\Pi}_0^{AB}\\ \overline{\Pi}_0^{AB} & \overline{\Pi}_0^{BB}\end{pmatrix}. \tag{30}$$

Equation (29) then goes over to

$$\overline{\Pi}=\overline{\Pi}_0+\vec{\Pi}_0^T\hat{\mathbf{U}}\vec{\Pi}_0+\vec{\Pi}_0^T\hat{\mathbf{U}}\hat{\Pi}_0\hat{\mathbf{U}}\vec{\Pi}_0+\cdots. \tag{31}$$

The matrix products can be summed to give

$$\overline{\Pi}=\overline{\Pi}_0+\vec{\Pi}_0^T\hat{\mathbf{U}}\sum_{n=0}^{\infty}[\hat{\Pi}_0\hat{\mathbf{U}}]^n\vec{\Pi}_0, \tag{32}$$

which can be evaluated as a matrix geometric series as

$$\sum_{n=0}^{\infty}[\hat{\Pi}_0\hat{\mathbf{U}}]^n=[\mathbf{1}-\hat{\Pi}_0\hat{\mathbf{U}}]^{-1}, \tag{33}$$

and Eq. (32) is calculated to yield

$$\overline{\Pi}=\overline{\Pi}_0^A+\overline{\Pi}_0^B-\frac{\tilde{u}_A(\overline{\Pi}_0^A)^2(1+\tilde{u}_B\overline{\Pi}_0^{BB})+\tilde{u}_B(\overline{\Pi}_0^B)^2(1+\tilde{u}_A\overline{\Pi}_0^{AA})-2\overline{\Pi}_0^A\tilde{u}_A\overline{\Pi}_0^{AB}\tilde{u}_B\overline{\Pi}_0^B}{(1+\tilde{u}_A\overline{\Pi}_0^{AA})(1+\tilde{u}_B\overline{\Pi}_0^{BB})-\tilde{u}_A\tilde{u}_B(\overline{\Pi}_0^{AB})^2}. \tag{34}$$

Equation (34) is the central result of this work and much of the further discussion will be based on its properties.

C. Limiting behavior

In order to test the usefulness of Eq. (34) it is necessary to investigate its behavior in various limits of disorder.

1. Weak disorder limit; uniform interaction

To establish a connection with formula (24) we first study the limit of low disorder and asymptotically equal bare contact interaction strengths $u^A=u^B=u$. It is well known [4] that in this limit the CPA self-energy goes over to the virtual crystal limit $\Sigma_{c/v}\to cV_{c/v}$ and the vertex correction to $\Lambda\to c(1-c)V_cV_v$. Accordingly, the weights in the two-particle function defined in (16)–(18) go over to $\xi\to c$, $\eta\to(1-c)$, and $\gamma\to c(1-c)F_cF_v$. As a result of this it is possible to pull the two weights ξ and η multiplied with the unweighted two-particle function out of the energy convolution, since they are now independent of energy. The impurity weighted versions of the polarizability can therefore be expressed in terms of the unweighted function as $\overline{\Pi}^A=c\overline{\Pi}$ and $\overline{\Pi}^{AA}=c^2\overline{\Pi}+c(1-c)\Omega$, where $\Omega(i\omega)\equiv-\beta^{-1}\Sigma_{iz}F_c(iz)F_v(i\omega-iz)$. The behavior of the host weighted functions and the mixed one follow in analogy. Through inserting into (34) it is found that the scattering term factorizes as

$$\overline{\Pi}\to\overline{\Pi}_0-\frac{\overline{\Pi}_0u\overline{\Pi}_0(1+u\Omega)}{(1+u\overline{\Pi}_0)(1+u\Omega)}, \tag{35}$$

which is identical to (24).

2. Strong disorder or split band limit

In Ref. 5 we had shown explicitly that in the regime of strong disorder, when the widths of the single-particle bands become negligible compared to the disorder strengths involved, the mixed component of the CPA two-particle function K^{AB} go to zero whereas the double-weighted functions $K^{AA/BB}$ become effectively identical to the single-weighted ones $K^{A/B}$. The same behavior also translates to the weighted polarizabilities and therefore in this limit (34) goes over to

$$\overline{\Pi}=\frac{\overline{\Pi}_0^A}{1+\tilde{u}^A\overline{\Pi}_0^A}+\frac{\overline{\Pi}_0^B}{1+\tilde{u}^B\overline{\Pi}_0^B}. \tag{36}$$

Even though this already looks very similar to (27) it is not trivially the same. However we showed in Ref. 5 that in this limit

$$K^{A/B}\to x^{A/B}\sum_k G_{c\,\mathrm{crys}}^{A/B}(k)G_{v\,\mathrm{crys}}^{A/B}(-k)=x^{A/B}K_{\mathrm{crys}}^{A/B}, \tag{37}$$

where $x^{A/B}$ is the concentration c and $(1-c)$ of the A and B component, respectively, and the subscript ''crys'' is chosen to label the corresponding two-particle functions of the pure A and B media. This in connection with the definition of $\tilde{u}^A$ and $\tilde{u}^B$ from (28) finally shows that (27) and (34) are indeed identical in this limit.

3. General behavior

In order to examine the predictions that (34) makes for a general case, we introduce the following definitions:

$$\overline{\Pi}_0^A\equiv\chi\overline{\Pi}_0, \qquad \overline{\Pi}_0^{AA}\equiv\chi\zeta\overline{\Pi}_0+\Gamma, \tag{38}$$

where $\Gamma(i\omega)\equiv-\beta^{-1}\Sigma_{iz}\gamma(iz,i\omega-iz)$. Due to probability conservation the other weighted functions are defined as

$$\overline{\Pi}_0^B=(1-\chi)\overline{\Pi}_0, \quad \overline{\Pi}_0^{AB}=\chi(1-\zeta)\overline{\Pi}_0-\Gamma,$$
$$\overline{\Pi}_0^{BB}=(1-2\chi+\chi\zeta)\overline{\Pi}_0+\Gamma. \tag{39}$$

In a general case, the polarization weights χ and ζ are only very indirectly related to the original weights ξ and η for the unintegrated two-particle function K. They may assume different values for any particular energy at which the polarizability is considered and therefore they generally depend on energy. Inserting this into (34) we find that

$$\overline{\Pi}=\overline{\Pi}_0-\overline{\Pi}_0^2\{[\chi^2\tilde{u}^A+(1-\chi)^2\tilde{u}^B]+\tilde{u}^A\tilde{u}^B[\chi(\zeta-\chi)\overline{\Pi}_0+\Gamma]\}$$
$$\times\{1+[\chi\zeta\tilde{u}^A+(1-2\chi+\chi\zeta)\tilde{u}^B+\tilde{u}^A\tilde{u}^B\Gamma]\overline{\Pi}_0$$
$$+(\tilde{u}^A+\tilde{u}^B)\Gamma+\tilde{u}^A\tilde{u}^B\chi(\zeta-\chi)\overline{\Pi}_0^2\}^{-1}. \tag{40}$$

If this this is compared to a corresponding Dyson equation for the polarizability with a renormalized self-energy-like expression M:

$$\overline{\Pi}=\overline{\Pi}_0+\overline{\Pi}_0M\overline{\Pi}, \tag{41}$$

this expression M, which can also be viewed as a disorder average ''dressed'' interaction, is found to be

$$M=-\frac{[\tilde{u}^A\chi^2+(1-\chi)^2\tilde{u}^B]+\tilde{u}^A\tilde{u}^B\chi(1-\chi)\Phi}{1+[\tilde{u}^A+\tilde{u}^B]\chi(1-\chi)\Phi}, \quad (42)$$

where we had introduced $\Phi=[\chi(\zeta-\chi)\overline{\Pi_0}+\Gamma]/[\chi(1-\chi)]$. Introducing a generalized energy dependent average interaction strength

$$\bar{u}=\chi^2\tilde{u}^A+(1-\chi)^2\tilde{u}^B, \quad (43)$$

and a generalized contact potential fluctuation strength

$$\Delta=\chi\tilde{u}^A-(1-\chi)\tilde{u}^B, \quad (44)$$

Eq. (42) can be rewritten as

$$M=-\bar{u}+\frac{\chi(1-\chi)\Delta^2\Phi}{1+[\bar{u}+\Delta(1-2\chi)]\Phi}. \quad (45)$$

Finally introducing the renormalized function $\Psi=\Phi/(1+\bar{u}\Phi)$ one obtains

$$M=-\bar{u}+\frac{\chi(1-\chi)\Delta^2\Psi}{1+\Delta(1-2\chi)\Psi}. \quad (46)$$

We argue that this result represents a generalized form of an average T matrix approximation (ATA) of the polarizability of the medium with respect to the disordered contact potential relative to its ''mean'' background value $\bar{u}$ which is taken as the basis of an energy dependent background medium similar to a virtual crystal (VCA) energy. To motivate our comparison more, we recapitulate the main features of the ATA for a single particle propagator G in a binary disordered medium with on-site potentials $-\varepsilon^A$ and $-\varepsilon^B$ on the A and B components, respectively. The contact potentials have been defined with a negative sign here to match the definition of u^A and u^B from before, which were introduced as attractive interactions on an equivalent footing. The averaged T matrix equation for G can be written as

$$\bar{G}=\bar{G}_0+\bar{G}_0\bar{T}\bar{G}_0, \quad (47)$$

in which $\bar{G}_0$ is the virtual crystal propagator

$$\bar{G}_0=\frac{g}{1+\bar{\varepsilon}g}, \quad (48)$$

where we have set $\bar{\varepsilon}=c\varepsilon^A+(1-c)\varepsilon^B$ and g is the the propagator for a medium without the on-site potentials. The average T matrix $\bar{T}$ is defined as

$$\bar{T}=\frac{-c[\varepsilon^A-\bar{\varepsilon}]}{1+[\varepsilon^A-\bar{\varepsilon}]F_0}+\frac{-(1-c)[\varepsilon^B-\bar{\varepsilon}]}{1+[\varepsilon^B-\bar{\varepsilon}]F_0}, \quad (49)$$

where $F_0=\bar{G}_0(m,m)$. Introducing furthermore $\delta=\varepsilon^A-\varepsilon^B$, the corresponding ATA self-energy Σ_{ATA} relating g and G can be written as

$$\Sigma_{\mathrm{ATA}}=-\bar{\varepsilon}+\frac{\bar{T}}{1+\bar{T}F_0}=-\bar{\varepsilon}+\frac{c(1-c)\delta^2F_0}{1+(1-2c)\delta F_0}. \quad (50)$$

The aforementioned analogy hence builds on the correspondence of the quantities

$$\begin{aligned} \bar{\varepsilon} &\leftrightarrow \bar{u}, & \delta &\leftrightarrow \Delta, \\ g &\leftrightarrow \overline{\Pi_0}, & \Sigma_{\mathrm{ATA}} &\leftrightarrow M, \\ \bar{G} &\leftrightarrow \overline{\Pi}, & F_0 &\leftrightarrow \Psi. \end{aligned} \quad (51)$$

This correspondence becomes exact in the asymptotic limits discussed before and continues to hold qualitatively in an intermediate regime. The difficulty in finding a rigorous comparison in the most general case stems again from difficulty of finding general expressions for the energy dependence of the integral weights χ and ζ and the integrated diagonal correction term Γ.

The reason why our weighted scattering expansion can be expected to yield a better result than an undifferentiated decoupling of the Dyson equation for the contact potential, as it is shown to do by our numerical calculations in the next section, can be understood from the argument that averages over higher moments of Π_0 which occur in this expansion such as $\langle\Pi_0^2\rangle$ and $\langle\Pi_0^3\rangle$ are better approximated by a decoupling as $\langle\Pi_0^2\rangle\simeq(\overline{\Pi_0^A})^2/c+(\overline{\Pi_0^B})^2/(1-c)$ and $\langle\Pi_0^3\rangle\simeq(\overline{\Pi_0^A})^2\overline{\Pi_0^{AA}}/c^2+2\overline{\Pi_0^A}\overline{\Pi_0^B}\overline{\Pi_0^{AB}}/c(1-c)+\overline{\Pi_0^{BB}}(\overline{\Pi_0^B})^2/(1-c)^2$ rather than $\langle\Pi_0^2\rangle\simeq\overline{\Pi_0^2}$ and $\langle\Pi_0^3\rangle\simeq\overline{\Pi_0^3}$, respectively, because the former approximation reduces a wrong weighting and overcounting of scattering processes that the latter approximation erroneously infers.

IV. NUMERICAL RESULTS

In this section we discuss a numerical implementation of our previous results within a commonly used model in three-dimensional systems. Rather than attempting a direct comparison to experimental data, which would require us to confine ourselves to a very narrow parameter region, it shall be our particular priority in this section to exemplify and visualize how the theory developed here correctly predicts the formation of excitons also in intermediate regimes of disorder, where other theories to date fail to work, by running through a wide range of parameters.

Since within the quasi-ATA contact potential model of the electron-hole interaction the excitonic polarizability can be obtained directly by inserting the weighted components of the average polarizability for the free particle system into Eq. (34), we draw strongly from the results obtained for the non-interacting system in Ref. 5. The main input necessary for the numerical implementation of a single-site CPA are the single-particle densities of states for the conduction and valence band. As in Ref. 5 we take

$$\begin{aligned} \rho_\mu(E)&=\frac{2}{\pi w_\mu^2}\sqrt{w_\mu^2-E^2}, & |E|&\leq w_\mu, \\ \rho_\mu(E)&=0, & |E|&\leq w_\mu. \end{aligned} \quad (52)$$

It is well known that this density of states does not exhibit any of the finer structure of a real system, but it includes the more global features of a wide class of systems giving a finite bandwidth and the appropriate van Hove singularities at the band edges. Moreover, it matches well with the spirit of a single-site CPA which, even though it reproduces the global influence of disorder on the system correctly in all regimes, cannot account for more detailed structure brought about by the scattering of particles off clusters of impurities

which usually involve momentum dependent self-energy contributions whose evaluation would require a more specific knowledge of the single-particle dispersion laws.

For amalgamation-type solid solutions, i.e., alloys whose densities of states of the pure A and B substances overlap to a great extent in the respective conduction and valence bands, CPA results already exist[4] for the case $u_A = u_B = u$. We shall therefore focus on the region of parameters which corresponds to intermediate disorder, where our approximation provides significantly better results than earlier approaches. A restriction to a rather specific region of parameter space becomes necessary since we now have six independent parameters which govern the behavior of our spectra, i.e., the concentration c, the relative valence conduction bandwidth w_v/w_c, the disorder strengths V_c and V_v in the respective bands and the corresponding disordered contact interaction strengths u_A and u_B, accounting for the dynamic part of the electron-hole correlations.

In determining the region of interest we note that, as pointed out by many workers (cf. for example the review article by Rashba[10]), the CPA produces a ''pseudo'' gap in the single-particle DOS at all concentrations once the disorder strengths exceed the half-width of the single-particle bands involved, $V_\mu \geq w_\mu$, which also translates to the joint DOS in some regimes. In more realistic systems, however, usually a true gap only exists once the disorder strengths exceed the full bandwidths $V_\mu \geq 2w_\mu$, even though in the regime $2w_\mu \geq V_\mu \geq w_\mu$ the number of states in the region of the pseudogap is strongly suppressed. Because of this, we shall concentrate our attention to the beginning region of the true gap behavior and choose $|V_\mu| = 3w_\mu$.

In calculating the absorption spectra, we have first obtained the weighted components of the polarizability without electron-hole interactions. Figures 2(a), 2(b) and 4(a), 4(b) show the real and negative imaginary part of $\overline{\Pi}_0$ and all its decompositions into single- and double-weighted components for parallel disorder, $\mathrm{sgn}(V_c) = \mathrm{sgn}(V_v)$, and antiparallel disorder, $\mathrm{sgn}(V_c) = -\mathrm{sgn}(V_v)$, respectively. Specifically, the conduction and valence band disorder have been chosen to be $V_c = 3.0$ and $V_v = \pm 2.4$ in connection with the half-bandwidths $w_c = 1.0$ and $w_v = 0.8$. It should be noted that all energies occurring in our results effectively scale with the half-width of the conduction band w_c as it is normalized to unity.

We can see from Figs. 2(b) and 4(b), that in the region of parameters considered, the joint density of states has already split quite clearly into distinct A and B parts for both cases of disorder and the difference of the double- and single-weighted components has become relatively small due to the dominance of the total diagonal matrix elements of the two-particle function in this regime. Note that in all the figures for the noninteracting polarizability only the single AB function has been plotted and the components of the spectra sum as $\overline{\Pi}_0^{A/B} = \overline{\Pi}_0^{AA/BB} + \overline{\Pi}_0^{AB}$ and $\overline{\Pi}_0 = \overline{\Pi}_0^{AA} + \overline{\Pi}_0^{BB} + 2\overline{\Pi}_0^{AB}$.

In the case of parallel disorder of Fig. 2(b), the joint DOS is divided up into into a central bulk part which is mainly constituted from AA and BB transitions and a separate set of flanks on either side of it, which contain a notable amount of AB transitions. In the case of antiparallel disorder of Fig. 4(b), on the other hand, it decomposes into two separate parts with a pronounced gap between them, whereby the upper part consists mainly of AA and the lower part of BB transitions. Even though the joint function appears to be very close to zero in the gap region for this case, we discover a finite contribution of double-weighted components centered between the split bands.[5] These states can be considered ''mute'' in the absence of any electron-hole interaction since cumulatively they do not contribute to the polarization.

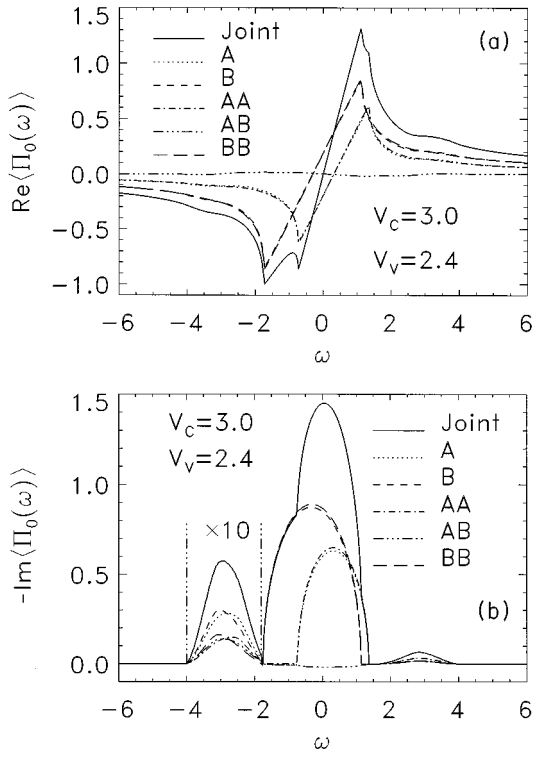

FIG. 2. (a) Real and (b) negative imaginary parts of the noninteracting polarizability for parallel disorder at $c = 0.35$. All energies scale with the conduction half-band width w_c which has been set to unity, $w_c \equiv 1$, while w_v is taken to be $w_v = 0.8$. Since this spectrum is taken at disorder strengths $V_c = 3.0$ and $V_v = 2.4$, i.e., at the beginning of the true gap region of the CPA, the single- and double-weighted functions coincide to a great extent, and two flanks of the spectra which to a substantial degree contain mixed AB components have split off sideways [cf. the lower end of the joint DOS in (b) where the values were enlarged by a factor of 10]. However, it becomes clear from the spectra in Fig. 3 that the residual interference of A and B absorption amounts to a significant influence on the excitonic absorption as the corresponding electron-hole interactions are introduced.

It appears from these results as if the system is already very close to the strong disorder asymptotic behavior where the split components are essentially independent, but we shall find that this is indeed not the case, agreeing with the result of Onodera and Toyozawa[11] who state that this regime is reached only beyond a relative disorder strength of about $V_\mu/w_\mu = 10$. If in the interacting case states are pulled down from the upper band into this region by means of the electron-hole interaction, they will experience a significant broadening and hence change the excitonic absorption in a large region as as will be apparent from the plots in Fig. 5.

In order to show the effect of the various components of

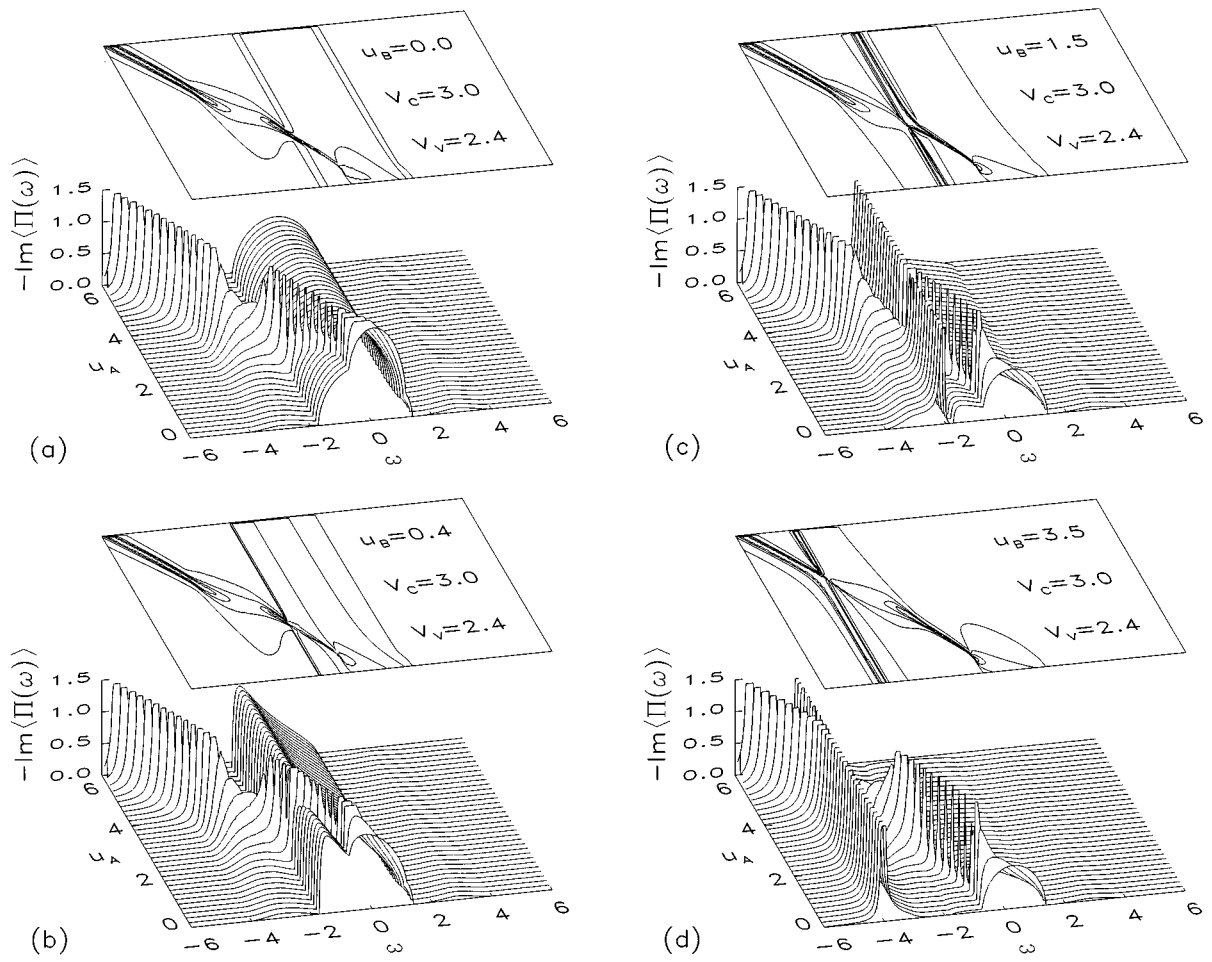

FIG. 3. Excitonic absorption spectra created by means of Eq. (34) from the weighted components of the noninteracting spectrum in Fig. 2. In each of the plots (a), (b), (c), (d) the contact potential strength u_B associated with B atoms is kept at a constant value while u_A is increased from 0 to 6 from the front to the back of the set of overlayed plots. The overlayed contour plots show the paths and broadenings of the excitons as the parameter strengths are varied. The contour lines are taken at level heights of 0.1, 0.5, 1.0, 1.5, respectively. Comparing the plots (a) $u_B=0.0$, (b) $u_B=0.4$, (c) $u_B=1.5$, (d) $u_B=3.5$, one can see that mutual interference effects of both interactions are relatively small. The main such interference effect is that B resonance attains some broadening once the A resonance has passed it, cf. (c).

the densities of states on the formation of excitons in a concise way we have plotted stacks of three-dimensional overlays of the obtained spectra. In every separate stack of the spectra in Figs. 3(a)–3(d) and 5(a)–5(d) the strength u_B of the contact interaction on a B site of the alloy — here associated with the lower lying component — is kept constant whereby the interaction strength u_A on an A site — associated with the higher lying component — is varied through an interval of strengths from zero to a value where it is sufficiently large to pull the exciton below the lowest component of the contributing unperturbed joint density of states. The same procedure is performed over all stacks of plots in Figs. 3 and 5 as u_B is gradually increased through a similar interval of values as u_A.

Although, in an experimental situation it would probably be much easier to vary such parameters of the system as the concentration and to some extent also the strengths of the disorder by using different substances for the production of the solid solutions, a strong variation of the contact potential strengths u_A and u_B is better suited for a theoretical study of the global features of the excitonic absorption predicted by our model. As a result we are able to analyze the excitonic absorption through a whole region of the three-dimensional parameter space spanned by ω, u_A, and u_B. In addition, since it is difficult to find a view-angle of the resulting plots which shows all features of the spectra simultaneously, we have cut off the resonance peaks at an appropriate value and overlayed a contour representation of the spectra which renders more detailed information about the position and the width of the excitonic resonances as the interaction strengths are increased.

As can already be seen from Eq. (34), the width of the resonances will be largely determined through the behavior of the double-weighted components, i.e., through the magnitude of the imaginary parts of $\overline{\Pi}_0^{AA}$ and $\overline{\Pi}_0^{AB}$ as well as $\overline{\Pi}_0^{BB}$ and $\overline{\Pi}_0^{AB}$ at the solutions of $\mathrm{Re}[\overline{\Pi}_0^{AA}]=-1/\tilde{u}_A$ and of $\mathrm{Re}[\overline{\Pi}_0^{BB}]=-1/\tilde{u}_B$, respectively. This implies that it is possible to have a very sharp resonance of the exciton peak associated with the higher lying component of the joint DOS deep within the region where the DOS is relatively large, but almost entirely consists of the opposite component. On the

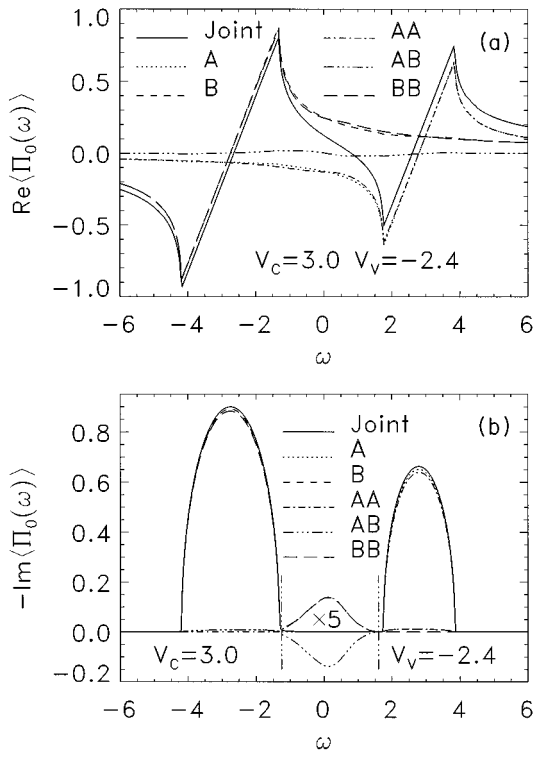

FIG. 4. (a) Real and (b) negative imaginary parts of the noninteracting polarizability for antiparallel disorder and parameters $c=0.35$, $V_c=3.0$, $V_v=-2.4$, $w_c=1.0$, and $w_v=0.8$. The antiparallel direction of the band offsets causes the imaginary part (joint DOS) in (b) to split into two distinct components mainly constituted by A and B transitions, respectively, separated by a wide gap. Even though the cumulative function is very close to zero in the central region, the double-weighted components are finite there [cf. the central region in (b) where the values were enlarged by a factor of 5] and hence they lead to a substantial broadening if an excitonic resonance is pulled out of the higher lying A component into this region, as can be seen from the excitonic spectra in Fig. 5.

other hand the resonance can be very broad even in a region where the cumulative DOS is practically zero, due to the presence of finite double-weighted components which mutually cancel out to a great extent, once they are summed.

In Fig. 3(a) the set of spectra commences with the completely unperturbed joint DOS for parallel disorder in Fig. 2. The A exciton which is being pulled out at the lower end of the central bulk part, which consists almost entirely of AA and BB components, becomes very sharp as soon as it leaves the pure A component at about $\omega=-0.7$ corresponding to an A interaction strength $u_A=0.45$. Beyond this value almost the entire oscillator strength of the A component is found in the resonance and thus only the pure B contribution remains in the central part as u_A is increased further. It should be noted that these resonances show a finite width also when they are exterior of any of the DOS contributions due to a small artificial imaginary part of about 10^{-3} units which has been added to the energy in order to ensure the correct analyticity of the quantities involved at the given numerical accuracy. A major broadening occurs subsequently as the resonance crosses the lower AB region which sharpens again once it has passed its lower end. The overlayed contour plot suggests that in the region without almost any AA states, the increase of the excitonic binding energy is throughout linear with the increase to the interaction strength u_A. However, as the bound state passes through the the lower split off flank, which is constituted of about 50% $AB-$ and 25% AA and BB components, respectively, see the $10\times$ enlarged region in Fig. 2(b), it gets broadened and the propagation path of the bound state seems to attain a parallel shift (of about $\omega=0.7$) with respect to the initial one, corresponding to a constant addition to the binding energy beyond the lowest flank of the spectrum. This additional deepening of binding is found through all stacks of spectra for parallel and antiparallel disorder equally. It can be observed throughout Figs. 3(b)–3(d) that as the A resonance passes the lower AB flank most of the states from this region are being absorbed into the resonances while the same is true for the the upper AB flank of the spectrum which feels the effect from afar. A very similar behavior is observed as u_B is increased over the series of stacked plots and the last bits of the upper flank get absorbed in this process. Passing through the lower AB flank also gives a strong broadening which accounts for the persistence of B states which are not influenced by the A interaction.

The plots also show that the formation of excitonic states associated with either of the underlying components of the alloy is largely independent of correlations between the two interaction strengths u_A and u_B, i.e., the formation of bound states associated with one of the two material components is seen to be as good as unaffected by a variation of interaction strength associated with the complementary component. The only slight correlation which comes into play is via the mixed AB components to which both u_A and u_B couple weakly. It can be observed that as the resonance associated with the higher lying component passes through the shifted body of the lower lying one, both this resonance and the peak width of the absorption edge narrow in the case of parallel disorder Figs. 3(b)–3(d) and broaden in the case of antiparallel disorder Figs. 5(b)–5(d).

Figures 5(a)–5(d) for antiparallel disorder exhibit many similar properties to the ones for the parallel case, but they also display quite a few novel features. The A resonance is strongly broadened as it is pulled into the center of the gap, which the noninteracting absorption for this case from Fig. 4(b) exhibits. This broadening stems from the AA and BB components which still prevail in this region and which are compensated by the AB gain contribution, see the $5\times$ enlarged region of Fig. 4(b). It is very curious to observe however, that even after the resonance has passed to lower energies, there is a finite hump remaining in the gap center which is subsequently bleached as the B resonance also shifts downwards. The development of this hump can be followed through Figs. 5(a)–5(d) if one looks through the trough that the A resonance forms in the central region of the gap onto the residual spectrum visible at the back. It mainly consists of BB states which remain in this region whereas both the AA and AB components become largely withdrawn. Looking at the contour plots of this arrangement suggests that, in addition to the constant increase in binding of the B resonance as u_B increases, which is comparable in magnitude to the one observed for parallel disorder as the central AB re-

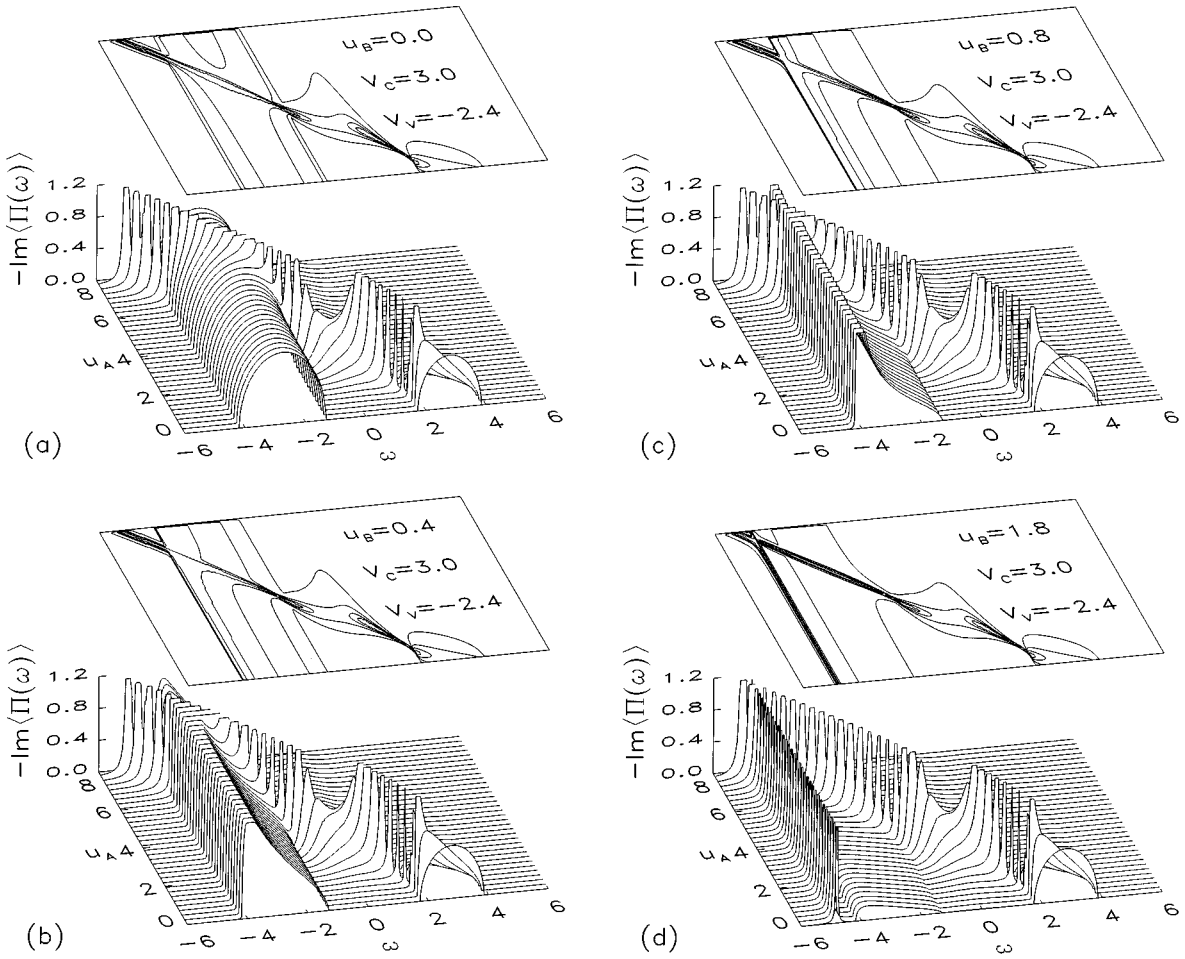

FIG. 5. Excitonic absorption spectra based on the noninteracting spectrum in Fig. 4. While in each of the plots (a), (b), (c), (d) u_A is varied from 0 to 8 to pull the A resonance below the onset of the lowest B states, u_B is varied as (a) $u_b=0.0$, (b) $u_B=0.4$, (c) $u_B=0.8$, (d) $u_B=1.8$. Opposite to the parallel case shown in Fig. 3 the interference of the two interactions amounts to a narrowing of the B type resonance as the A resonance passes it, cf. (c). Both here and for the cases shown in Fig. 3 this can be understood to originate from the mixed AB contribution into which both u_A and u_B couple weakly. Similar to Fig. 3 the contour lines are taken at level heights of 0.1, 0.4, 0.8, 1.2, respectively. Note also that an unweighted contact potential model with a uniform interaction u of Eq. (24) would in this case erroneously predict a trapping of an excitonic resonance in the gap region where $\mathrm{Re}[\overline{\Pi}_0]=0$ at about $\omega=0.8$, as $u\to\infty$.

gion is passed, the constant of proportionality for the deepening seems to have increased corresponding to a faster linear deepening of the A exciton binding with increasing u_A.

The spectra of Figs. 5(a)–5(d) are also particularly suitable to visualize that a weighted scattering expansion used in the context of an average decoupling and a contact potential model with two distinguishable interaction strengths renders a much more accurate prediction for the formation of the excitonic resonances than the unweighted one of Eq. (24). Equation (24) produces a resonance whenever $\mathrm{Re}[\overline{\Pi}_0]=-1/u$ and $\mathrm{Im}[\overline{\Pi}_0]$ is small or zero. In a split band case as shown in Fig. 4 the real part is seen to have a zero in the gap where $\mathrm{Im}[\overline{\Pi}_0]\simeq 0$. This means that an increase of the interaction strength u would lead to a bound state being trapped between the split bands at this zero of $\mathrm{Re}[\overline{\Pi}_0]$ in the limit $u\to\infty$. This behavior of course is clearly wrong, since one can expect that the binding energy of any occurring excitonic resonance deepens, in this case the binding energy of the resonance associated with the higher lying A band, as the interaction strength increases. This failure in giving the right asymptotic description can be ascribed to a misweighting and overcounting even of scattering processes which contain two-particle correlations only. Our approximation overcomes this problem to a great extent and it is void of the erroneous trapping of the resonance, which as expected passes on to lower energies and finally appears below the B band as u_A is increased, independently of the value of u_B.

The variation range of the carrier interaction strengths, particularly the one for u_A, which we have plotted throughout Figs. 3 and 5 is very large and is unlikely to be found in semiconductor alloys. However, mixtures of molecular crystals, and mixed crystals of rare gases,[12] which form quite narrow bands and at the same time have rather strong band offsets,[13] might be candidates for such behavior. Unfortunately, experimental work on the spectra of mixed rare gas solids has only been reported in relatively narrow regions, where only one of the substances exhibits the interesting exciton lines, whereas the corresponding features of the other component lie outside the captured region.[14,15] This makes a quantitative comparison of these results with the theory presented here unrewarding.

V. COMPARISON TO EARLIER WORK

Much earlier work on excitons in strongly disordered binary solid solutions at finite concentrations focussed on systems where the exciton is tightly bound with a binding energy greater that the narrow bandwidth. In this case the Frenkel exciton has been frequently described by a ''single''-particle Green's function based on the theory of molecular excitons by Davydov.[16] One of the standard assumptions within this framework is that the matrix elements in the optical absorption, $m_{\mathbf{k},\mathbf{k}'}=\langle c,\mathbf{k}|\hat{\varepsilon}\cdot\mathbf{p}|v,\mathbf{k}'\rangle$ are strongly localized in momentum space, i.e., $m_{\mathbf{k},\mathbf{k}'}=\text{const}\times\delta_{\mathbf{k},\mathbf{k}'}\delta_{\mathbf{k},0}$ which means that the contributing transitions are not only required to be vertical due to the approximate absence of total momentum of the exciting photon but also to only occur at one single point in the bands at $\mathbf{k}=\mathbf{k}'=0$ (Davydov component), due to the momentum of the relative electron-hole motion being approximated to zero.

Early treatments of the absorption of mixed molecular crystals employed the average amplitude approximation (AAA) first introduced by Broude and Rashba,[17] which is able to roughly predict the position and gravity center strengths of the dominant transitions only. With the introduction of the CPA, which has some important advantages over the AAA, such as being able to produce an approximation of the actual shape of the joint DOS, it became possible to implement the Davydov theory within a self-consistent framework.

This has been pursued by Onodera and Toyozawa[11] and a little later by Hong and Robinson[18] who implemented the CPA as a single exciton band theory and tried to model their results particularly on observations made in experiments[19,20] on naphtalene and anthracene. In the early 1970s Sen realized that the spectra of alkali and cuprous halides were modified through spin-orbit splitting of the valence band and found that the situation can be better addressed using a two-channel exciton band theory with band mixing[21] which he compared to experimental spectra in $CuCl_cBr_{1-c}$,[22] $KCl_c\,Br_{1-c}$,[23–25] and $K_cRb_{1-c}Br$.[25] This two-channel exciton band theory, however, does not correspond to a genuine two-particle theory including vertex corrections, although Sen had also worked on the latter at that time for other purposes.[26,27]

The approaches of all the authors of Refs. 11, 18 and 21, despite their self-consistency, result in serious restrictions to the predictions their models can render about aspects of genuine two-particle behavior. They seem to give reasonable predictions on some of the features of Frenkel excitons in the strongly insulating substances, such as the movement of the exciton peaks as the concentration of the alloy is varied, when the calculated positions of the Davydov components are compared with the ones of the experimentally observed peaks in the absorption spectra.

A significant disadvantage of exciton band theories in general is that they only truly work if there is no disorder in the system such that the relative carrier motion decouples from the center of mass part. Once disorder is introduced this decoupling fails to work, corresponding to a continuous breaking of the k selection rule, and only a properly vertex corrected configurational averaging procedure on a two-particle level can overcome this difficulty.[5] Moreover, only one ''joint density of states'' bandwidth and disorder strength can be considered, rather than two independent values for both of these parameters, associated with the underlying conduction and valence bands. A behavior of the joint density of states as displayed for parallel conduction-valence band disorder which can lead to the filling of the central part of the joint DOS by the states arising from the AA and BB transitions even in a split band limit, as shown in Fig. 2, could for example never be obtained in such a simple single-particle picture. In none of the aforementioned references is the electron-hole interaction considered, so that the binding energy of the excitons and therefore their spacing from the continuum absorption edge, a particularly striking feature with Frenkel excitons, cannot be properly accounted for in any way. For the case of the weakly bound Wannier excitons such as occur in many semiconductor alloys, the only early work is found in a paper by Mahanti,[28] which, however, is largely phenomenological and primarily seeks to make predictions about how the linewidths of the exciton resonances, a property which is not well represented in any CPA theory of absorption, may be derived from the single-particle lifetimes involved.

The first work known to us, which is based on the treatment of a proper two-particle theory, is the paper by Abe and Toyozawa[9] who employed Velický's two-particle CPA (Ref. 3) to calculate the absorption in a noninteracting system with Gaussian disorder. Kanehisa and Elliott[4] thereafter considered both a two-particle CPA for the disorder and a contact interaction as a model for an electron-hole interaction, but they were only able to obtain an asymptotic solution in the regime of weak disorder, using the average decoupling of the unweighted polarizability in (24). As they pointed out, their results can be regarded as applying to the amalgamation regime and a comparison was made with experiments on III-V alloys such as $In_cGa_{1-c}P$,[29] $Ga_c\,Al_{1-c}As$,[30] and $GaAs_{1-c}\,P_c$.[31] Since these substances are all clearly within the amalgamation limit in which our results converge to formula (24), the same comparison holds for our theory in this limit and we do not attempt here to repeat it.

One should note that the approaches of Refs. 9, 4, 5, and the present work make the assumption that the optical matrix elements are constant over the single-particle bands involved, even though only vertical transitions at $\mathbf{k}=\mathbf{k}'$ are allowed, which contrasts the Davydov theory used in the earlier theoretical models of Refs. 11, 18, 21, where only the zero-momentum component $\mathbf{k}=\mathbf{k}'=0$ is taken. In a more realistic situation, the appropriate matrix elements will exhibit a more general $\mathbf{k}$ dependence, but it does not present any conceptual difficulty to modify our present results to model such cases as well, provided the actual dispersion laws for the conduction and valence bands are known.

VI. CONCLUSION

The present work is the most extensive to date which treats the correlated motion of pairs of interacting particles in a disordered medium. It draws from the extension of the CPA to two-particle propagation developed by Velický[3] and its extension to weighted two-particle Green's functions given in our earlier paper.[5]

The model introduced here achieves a better but still approximate treatment of the interference between the effects

of impurity scattering and direct two-particle (electron-hole) interaction and it provides an interpolation scheme through all strengths of disorder as well as the possibility to include site dependent variations in the direct electron-hole interaction within an ATA-like framework. It is therefore most appropriate for systems where the disorder causes a small but distinct band splitting, where previous asymptotic models fail to work. There are many disordered systems where such interacting pairs of particles play an important physical role and we believe the method can be extended to such situations. Modeling the excitonic absorption provides a particularly obvious application.

It seems that compared to the amount of experimental data available for the strongly amalgamation type solid solutions such as III-V and II-VI semiconductor alloys, experiments on more strongly persistent-type substances, in which the interesting physical features of both components are captured in a single measurement, are not so numerous. With our present treatment we therefore also hope to encourage further experimental work in this direction.

ACKNOWLEDGMENTS

The authors would like to thank Dr. M. A. Kanehisa and C. Heide for reading the manuscript and making useful suggestions.

[1] P. Soven, Phys. Rev. **156**, 809 (1967).
[2] D.W. Taylor, Phys. Rev. **156**, 1017 (1967).
[3] B. Velický, Phys. Rev. **184**, 614 (1969).
[4] M.A. Kanehisa and R.J. Elliott, Phys. Rev. **B 35**, 2228 (1987).
[5] N.F. Schwabe and R.J. Elliott, preceding paper, Phys. Rev. B **53**, 5301 (1996).
[6] B. Velický, S. Kirkpatrick, and H. Ehrenreich, Phys. Rev. **175**, 747 (1968).
[7] R.N. Aiyer, R.J. Elliott, J.A. Krumhansl, and P.L. Leath, Phys. Rev. **181**, 1006 (1969).
[8] R.J. Elliott, Phys. Rev. **108**, 1384 (1957).
[9] S. Abe and Y. Toyozawa, J. Phys. Soc. Jpn. **50**, 2185 (1981).
[10] E.I. Rashba, in *Optical Properties of Mixed Crystals*, edited by R.J. Elliott and I.P. Ipatova (North-Holland, Amsterdam, 1988), p. 215.
[11] Y. Onodera and Y. Toyozawa, J. Phys. Soc. Jpn. **24**, 341 (1968).
[12] N. Schwentner, E.E. Koch, and J. Jortner, *Electronic Excitations in Rare Gases* (Springer, Berlin, 1985), pp. 54–60.
[13] R. Nürnberger, F.J. Himpsel, E.E. Koch, and N. Schwentner, Phys. Status Solidi B **81**, 503 (1977).
[14] R. Haensel, N. Kosuch, U. Nielsen, U. Rössler, and B. Sonntag, Phys. Rev. B **7**, 1577 (1973).
[15] N. Nagasawa, T. Karasawa, N. Miura, and T. Nanba, J. Phys. Soc. Jpn. **32**, 1155 (1972).
[16] A.S. Davydov, Sov. Phys. Usp. **7**, 145 (1964).
[17] V.L. Broude and E.I. Rashba, Sov. Phys. Solid State **3**, 1415 (1961).
[18] H.K. Hong and G.W. Robinson, J. Chem. Phys. **52**, 825 (1970).
[19] S.D. Colson and G.W. Robinson, J. Chem. Phys. **48**, 2250 (1968).
[20] H.K. Hong and G.W. Robinson, J. Chem. Phys. **54**, 1369 (1971).
[21] P.N. Sen, Phys. Rev. Lett. **30**, 533 (1973); Phys. Rev. B **8**, 5624 (1973).
[22] Y. Kato, C.I. Yu, and T. Goto, J. Phys. Soc. Jpn. **28**, 104 (1970).
[23] M. Watanabe, Y. Nakamura, Y. Nakai, and T. Murata, J. Phys. Soc. Jpn. **24**, 428 (1968).
[24] T. Murata and Y. Nakai, J. Phys. Soc. Jpn. **23**, 904 (1969).
[25] T. Murata, J. Phys. Soc. Jpn. **25**, 1632 (1968).
[26] P.N. Sen and M.H. Cohen, J. Non-Cryst. Solids **10**, 147 (1972).
[27] P.N. Sen, Phys. Rev. B **8**, 5613 (1973).
[28] S.D. Mahanti, Phys. Rev. B **10**, 1384 (1974).
[29] R.J. Nelson and N. Holonyak, Jr., J. Phys. Chem. Solids **37**, 629 (1976).
[30] B. Monemar, K.K. Shih, and G.D. Pettit, J. Appl. Phys. **47**, 2604 (1976); R. Dingle, R.A. Logan, and J.R. Arthur, Jr., Inst. Phys. Conf. Ser. **33a**, 210 (1977).
[31] R.J. Nelson, N. Holonyak, Jr., and W.O. Groves, Phys. Rev. B **13**, 5415 (1976); R.J. Nelson, in *Excitons*, edited by E.I. Rashba and M.D. Sturge (North-Holland, Amsterdam, 1982), p. 319.